INL/CON-23-75889-Revision-0

Drop Analysis of a Department of Energy Standard Canister Containing Fort Saint Vrain SNF 24138

March 2024

Devin D Imholte, Peter Sakalaukus

Changing the World's Energy Future

INL is a U.S. Department of Energy National Laboratory operated by Battelle Energy Alliance, LLC

DISCLAIMER

This information was prepared as an account of work sponsored by an agency of the U.S. Government. Neither the U.S. Government nor any agency thereof, nor any of their employees, makes any warranty, expressed or implied, or assumes any legal liability or responsibility for the accuracy, completeness, or usefulness, of any information, apparatus, product, or process disclosed, or represents that its use would not infringe privately owned rights. References herein to any specific commercial product, process, or service by trade name, trade mark, manufacturer, or otherwise, does not necessarily constitute or imply its endorsement, recommendation, or favoring by the U.S. Government or any agency thereof. The views and opinions of authors expressed herein do not necessarily state or reflect those of the U.S. Government or any agency thereof.

INL/CON-23-75889-Revision-0

Drop Analysis of a Department of Energy Standard Canister Containing Fort Saint Vrain SNF 24138

Devin D Imholte, Peter Sakalaukus

March 2024

Idaho National Laboratory
Idaho Falls, Idaho 83415

http://www.inl.gov

Prepared for the
U.S. Department of Energy
Under DOE Idaho Operations Office
Contract DE-AC07-05ID14517

Drop Analysis of a Department of Energy Standard Canister Containing Fort Saint Vrain SNF– 24138

D. Devin Imholte[1], Peter Sakalaukus[2]
[1]Idaho National Laboratory
[2] Pacific Northwest National Laboratory

ABSTRACT

DOE manages over 300 types of SNF, many of which are located at the INL site. Managing this large variety of SNF for storage, transportation, and disposal poses a challenge to DOE. The Idaho Cleanup Project and INL are collaborating on the DOE SNF Road-Ready Demonstration ("Road-Ready Demonstration"), which will develop and demonstrate the designs, technology, processes, and regulatory framework for packaging DOE-managed SNF for "road-ready dry storage." Road-ready dry storage (RRDS) is an SNF management concept in which SNF is packaged into dry, sealed canisters that are then placed in on-site storage in anticipation of later transport and disposition. The forward-looking goal of the Road-Ready Demonstration is to establish the foundation for a large-scale RRDS program at the INL site.

One critical aspect of RRDS is the ability to certify the DOE Standard Canister and its associated transportation package in accordance with 10 CFR 71 for offsite transportation. Depending on the SNF type and transportation strategy, DOE Standard Canisters may be required to maintain structural integrity under hypothetical accident scenarios (e.g., drop events). The DOE Standard Canisters have been tested and analyzed under various SNF loading configurations and accident drop events in support of the Idaho Spent Fuel Facility and other DOE programs; however, no analysis has yet been completed in support of the recently initiated Road-Ready Demonstration.

This paper presents preliminary results from a finite element analysis of the Ø45.7 cm × 4.6 m (Ø18 in. × 15 ft) DOE Standard Canister under the 9 m drop at 80 degrees off-vertical drop scenario considered in previous INL tests and analyses. It considers the Fort St. Vrain spent nuclear fuel loading configuration proposed for the Road-Ready Demonstration, uses updated material properties, and applies the strain-based acceptance criteria established in ASME Boiler and Pressure Vessel Code's Section III, Division 3 rules for storage and transportation spent nuclear fuel containments. This updated analysis is compared to previous DOE Standard Canister drop analyses. Preliminary results from the updated analysis show that certain regions of the containment exceed the allowable limits during the accidental drop event. However, these regions are limited to components performing a non-structural function. While further work on this analysis will be pursued, this analysis serves as the foundation for formal calculations used to support applicable certification efforts of the RRDS system at INL.

INTRODUCTION

The U.S. Department of Energy (DOE) manages over 300 types of spent nuclear fuel (SNF), many of which are located at the Idaho National Laboratory (INL) site outside Idaho Falls, Idaho. One management concept is to package the DOE-managed SNF at the INL site into dry, sealed canisters, which are then placed in onsite storage for later removal [1]. The canisters and associated packaging are designed to satisfy storage requirements and can be readily placed into a configuration that would satisfy transportation requirements and disposal requirements, without the need to re-open and/or repackage, for as long as may be needed until transportation for disposition. This management concept is known as "road-ready dry storage" (RRDS).

In establishing a large-scale RRDS program at the INL site, the DOE SNF Road-Ready Demonstration (formerly known as "DOE SNF Packaging Demonstration," referred to as "Road-Ready Demonstration" hereafter) will demonstrate the capability to implement RRDS by packaging DOE-managed SNF into DOE Standard Canisters (DOESCs), packing the DOESCs into over-canisters that resemble commercial multi-purpose canisters, placing the over-canister into a storage overpack, and placing the storage overpack on a cask pad. This over-canister will then be compatible with a transportation or storage system, such as a storage cask for interim storage or transportation package for off-site transport. These DOESCs are expected to remain sealed over the course of their storage, transportation, and emplacement for disposal. Additional detail regarding the Road-Ready Demonstration may be found elsewhere [2, 3].

The specific type of SNF chosen for the Road-Ready Demonstration are Fort St. Vrain (FSV) high temperature gas reactor fuel assemblies currently in dry storage at INL [4]. While various SNF loading configurations and drop analyses were performed for the DOESC, no updated analysis has been performed for this FSV loading configuration. Furthermore, no analysis of the DOESC has ever been performed according to the requirements of the American Society of Mechanical Engineers (ASME) Boiler and Pressure Vessel (B&PV) Code (referred to as the "ASME Code" herein). This ASME Code is listed as the preferred construction code for SNF transportation packages [5]. This paper will present preliminary results of a finite element analysis (FEA) of an FSV-loaded DOESC with updated material properties using ASME Code acceptance criteria and compare with a more recently performed DOESC drop analysis.

BACKGROUND

The DOESC was originally designed under the National Spent Nuclear Fuel Program (NSNFP) and DOE Office of Environmental Management as a sealed containment for the wide variety of DOE-managed SNF [6, 7]. The DOESC is a welded stainless steel enclosure that comes in four different sizes to accommodate the variety of DOE-managed SNF. The Road-Ready Demonstration has selected the Ø45.7 cm × 4.6 m (Ø18 in. × 15 ft) variation (Figure 1). The DOESC design was included in the NRC license applications for the Yucca Mountain geological repository [8] and the Idaho Spent Fuel (ISF) Facility – a facility designed for packaging and storage of Peach Bottom, Shippingport and Training, Research, Isotopes, General Atomics SNF [9]. However, neither were not realized as operational facilities. The Road-Ready Demonstration is the most recent effort to use the DOESCs [2, 3, 10, 11].

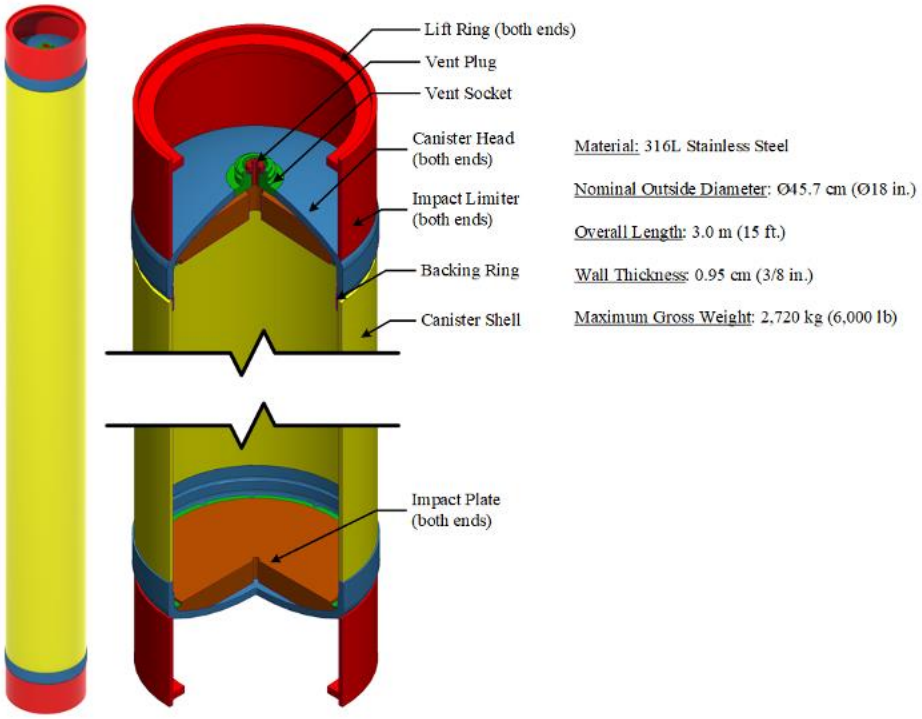

Figure 1: Empty DOESC, Ø45.7 cm × 4.6 m (Ø18 in. × 15 ft) variation.

Historical DOESC Drop-Testing and Analysis

The DOESC design has undergone rigorous full-scale drop-testing and post-drop analysis in support of the NSNFP and ISF programs [12, 13] (Figure 2). These drop-tests were performed for a combination of reasons. The DOESC serves as the containment barrier for some potentially damaged DOE-managed SNF—a barrier that cladding performs for undamaged commercial SNF during storage and transportation. This function required a robust canister design "that has significant safety margins for the known loads and safety margins for the loads that have been estimated" [7]. The 10 CFR 71.73 hypothetical accident drop events were used as a benchmark for the drop-tests, even though the DOESCs were intended for use within a vendor's SNF storage and transportation system. In addition to the 10 CFR 71 drop accidents, the Yucca Mountain repository-defined 7 m and 61 cm worst-orientation drops were also performed [6, 7, 13]. All the drop-tested DOESCs were shown via post-drop leak testing to maintain leaktight containment [12-14] (Figure 2). As part of these drop-testing campaigns, finite element models (FEMs) of the DOESCs different drop conditions were created and an FEA was executed to obtain results that were compared to the empirical results (Figure 3). Post-drop strain measurements in some locations were larger than those predicted with FEA. This led to the conclusion that the DOESC was capable of maintaining a leaktight containment under larger deformations than was simulated with FEA [13].

Figure 2: 1998 DOESC Drop-testing at Sandia National Laboratories, New Mexico (left) and INL (right) [13].

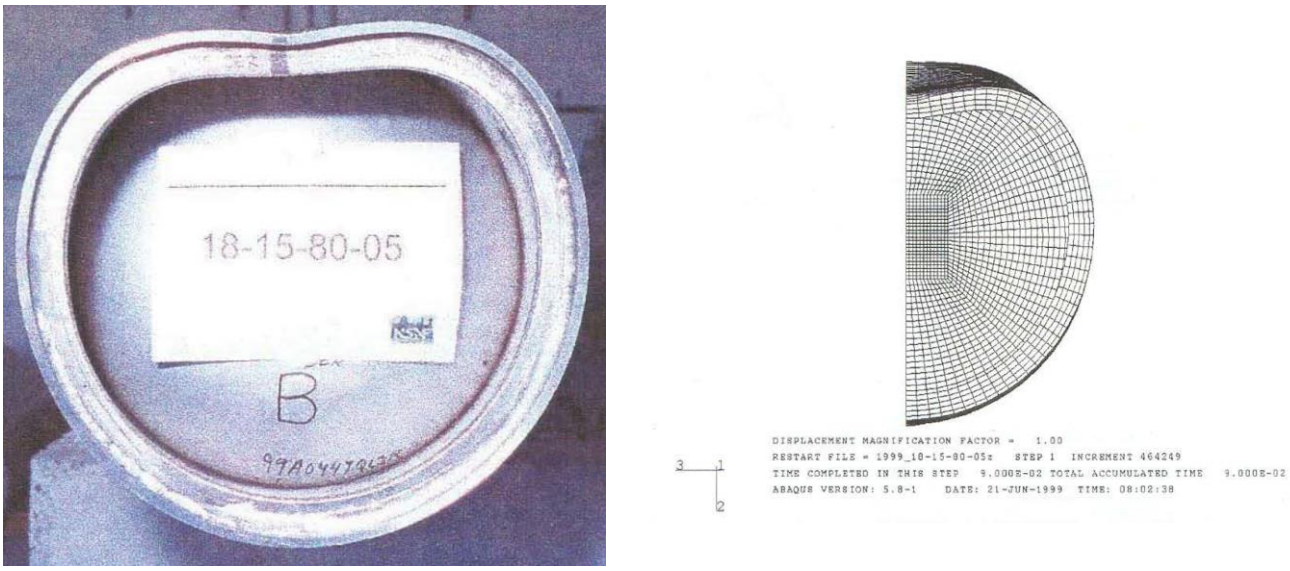

Figure 3: FEA of DOESC bottom head after 30 ft. drop (right) compared to empirical results (left) [13].

Road-Ready Demonstration DOESC Drop Analysis

The previous drop-testing campaigns demonstrated a robust DOESC design. These drop-tests were cited in the Yucca Mountain license application for the DOESC's performance during pre-closure [15]. While previous DOESC drop analyses were performed under a rigorous drop-testing campaign, there were two notable limitations of the associated FEA.

First, the acceptance criteria were limited to comparing the FEA-predicted deformations to the detailed post-drop deformations measured from the tested DOESC specimens [12, 13, 16]. While this provided a

means to establish strains from the drop-tested canisters and for comparison to particular regions of the DOESC, it is difficult to draw meaningful conclusions from plastic strains under different stress states. At the time of these initial drop-testing campaigns however, no ASME Code acceptance criteria existed for analyzing such energy-limited impact events. Section III Division 3 of the ASME Code was recently selected as the DOESC's construction code of record [17]. The Road-Ready Demonstration is considering 10 CFR 71 requirements for its RRDS. Therefore, it necessary to determine how the FSV-loaded DOESC performs during 10 CFR 71.73 accidental drops using the ASME Code's limits.

The second limitation of previous analyses was the lack of strain rate data. While quasi-static tensile properties are suitable for static structural analyses, using such data for dynamic impact events (e.g., accidental drops) can be overly conservative and overpredict failure. Previous DOESC drop analyses considered 20-70% increase in yield strength over quasi-static stress-strain data to account for dynamic strengthening for strain rates up to 200/sec [12, 13]. More recently, a 20% factor was deterministically applied to quasi-static true stress-strain data to account for strain rate behavior [16]. Recent analyses of other DOE SNF packages have applied detailed strain rate data for austenitic stainless steels at different strain rates and temperatures [18-21]. As such, an updated DOESC drop analysis should include such strain rate data for its 316L stainless steel containment.

To support the Road-Ready Demonstration, additional analysis is required to determine whether the DOESC can maintain containment following accidental drops. Building upon the successful DOESC drop-tests previously performed, this analysis therefore seeks to evaluate an FSV-loaded DOESC against the ASME Code's strain-based acceptance criteria using updated material strain rate properties.

In addition to performing an updated FEA, a comparison to the most recently performed FEA [16] of the DOESC is performed against ASME Code's strain-based acceptance criteria. This recently performed FEA considered DOESCs loaded with Peach Bottom SNF instead of FSV. However, since the SNF contents in neither situation were of interest, the comparison was made to evaluate how different SNF loading configurations affect the location and magnitude of the plastic strains in the containment boundary.

FINITE ELEMENT MODEL DESCRIPTION

Geometry

The DOESC FEM is developed using Abaqus CAE/Explicit 2021 [22] and executed using INL's Sawtooth high performance supercomputer. Abaqus/Explicit 2021 is validated for structural evaluations within Sawtooth [23].

The DOESC FEM is created based on the Ø25.7 cm (Ø18 in.) and 4.6-m (15-ft.) long ISF canister dimensions [16, 24]. The loading configuration for the DOESC assumed four FSV elements stacked within the basket and the shield plug stacked on top (Figure 4). Except for the retaining rings that hold the impact plates against the top and bottom heads, none of the internals are fastened to the DOESC containment. The orientation of the basket and internals considered for this analysis is falling onto the FSV element corners.

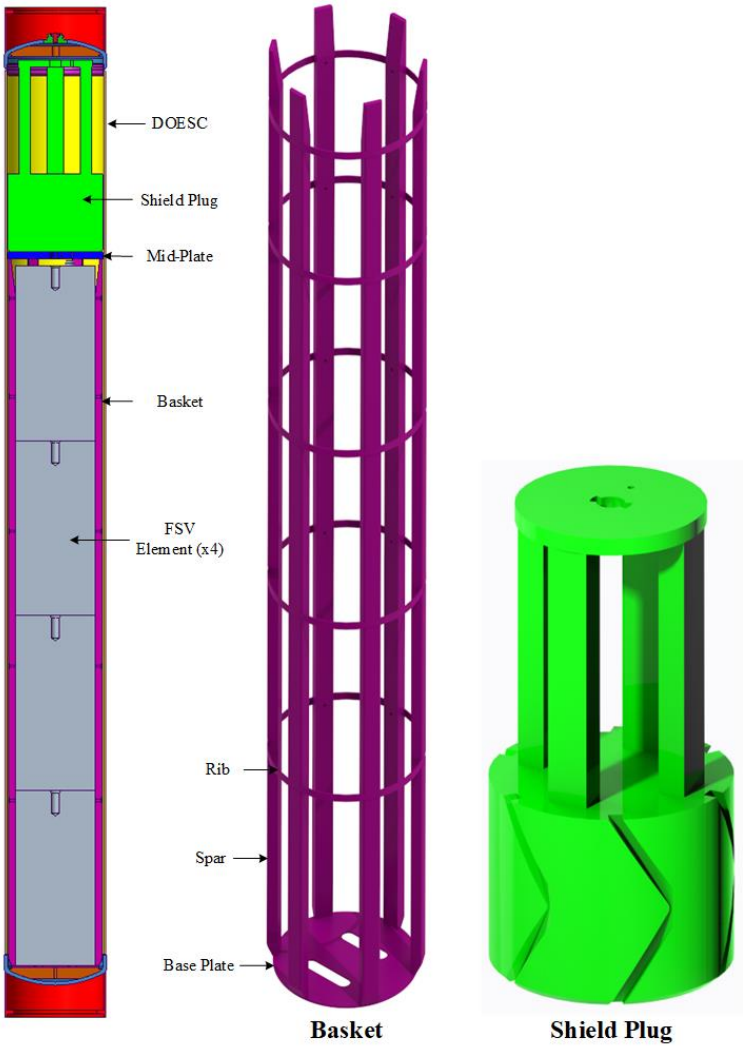

Figure 4: DOESC Loading Configuration.

Based on historical drop-tests of the Ø25.7 cm × 9 m (Ø18 in. × 15 ft.) DOESC, the 9 m (30 ft.) 80 degree off-vertical impact. In this configuration, the bottom impact limiter impacts first, which causes the top end of the canister to 'slapdown' onto the essentially unyielding surface. This slapdown was the drop event that resulted in the largest observed and predicted strains [12, 15]. Therefore, this analysis will only consider this drop height and DOESC impact orientation.

Contact surfaces are calculated at the beginning of the simulation. Compared to steel-steel coefficients of friction [25], a conservatively low friction coefficient of 0.3 is assigned to all surfaces, which minimizes energy dissipation from friction. This results in more kinetic energy dissipation by plastic deformation during the drop event.

Materials

The DOESC's entire containment (i.e., main shell, heads, impact limiters, lifting rings, impact plates) are constructed of 316L stainless steel. In addition, the basket (i.e., spars, ribs, mid-plate, and base plate) and shield plug are constructed of 316L stainless steel. All materials are modeled using true stress-strain relationships along with strain rate mechanical properties for 316L at room temperature [21, 26].

The FSV fuel elements are fabricated from H-327 and H-451 graphite [4]. However, the condition of the FSV elements following a drop event were not of interest for this analysis. Specifically, the containment boundary was the only area of interest during the drop simulation. Fuel configuration of the FSV fuel and the associated criticality are outside the scope of this paper, although previous analyses demonstrated this was not a concern for FSV fuel [4]. To represent realistic transfer of loads during the drop event, the FSV elements were modeled using the density for H-327 and H-451 graphite [4].

Although it is well-documented that weld material has lower uniform and fracture strain limits, weld material was not explicitly modeled at the welded joints for this analysis. Instead, welded joints were modeled as "ties" at the interfacing surfaces between components (e.g., head to main shell). Given the relatively low strains in the proximity of the weld joints (shown later), this assumption simplifies the analysis and is consistent with previous DOESC drop analyses [12, 13, 16].

Table 1 presents select mechanical properties for all materials.

Table 1. FEM Material Properties.

Component	**Material**	**Density (g/cc)**	**Modulus of Elasticity (MPa)**	**Poisson's Ratio**	**$\varepsilon_{fracture}$ (in./in. or mm/mm) [21]**	**$\varepsilon_{uniform}$ (in./in. or mm/mm) [21]**
Containment	316L Stainless Steel	8.02	195,121	0.31	1.94	0.46
Basket and Shield Plug						
FSV	H-327 Graphite	1.69		0.29	N/A	N/A

Meshing

The FEM was constructed entirely of eight-noded brick elements. Incompatible modes elements were used where possible due to their stability during kinetic impact (no hourglass control required) and stability under bending stress (i.e., heads, impact limiters, main shell, vent plug, vent socket, basket, FSV elements, shield plug). Reduced integration elements were limited to the impact plates and retaining rings where large plastic deformations were anticipated. The unyielding impact surface is modeled as an analytical rigid surface that is fixed in space. This approach is consistent with previous DOESC structural FEMs [16]. Figure 5 shows the assembly mesh of the entire FEM, with a total of 453,130 brick elements. Due to model symmetry of loading, materials and geometry, the DOESC and its contents are half-modeled, which is consistent with previous analyses [12, 13, 16].

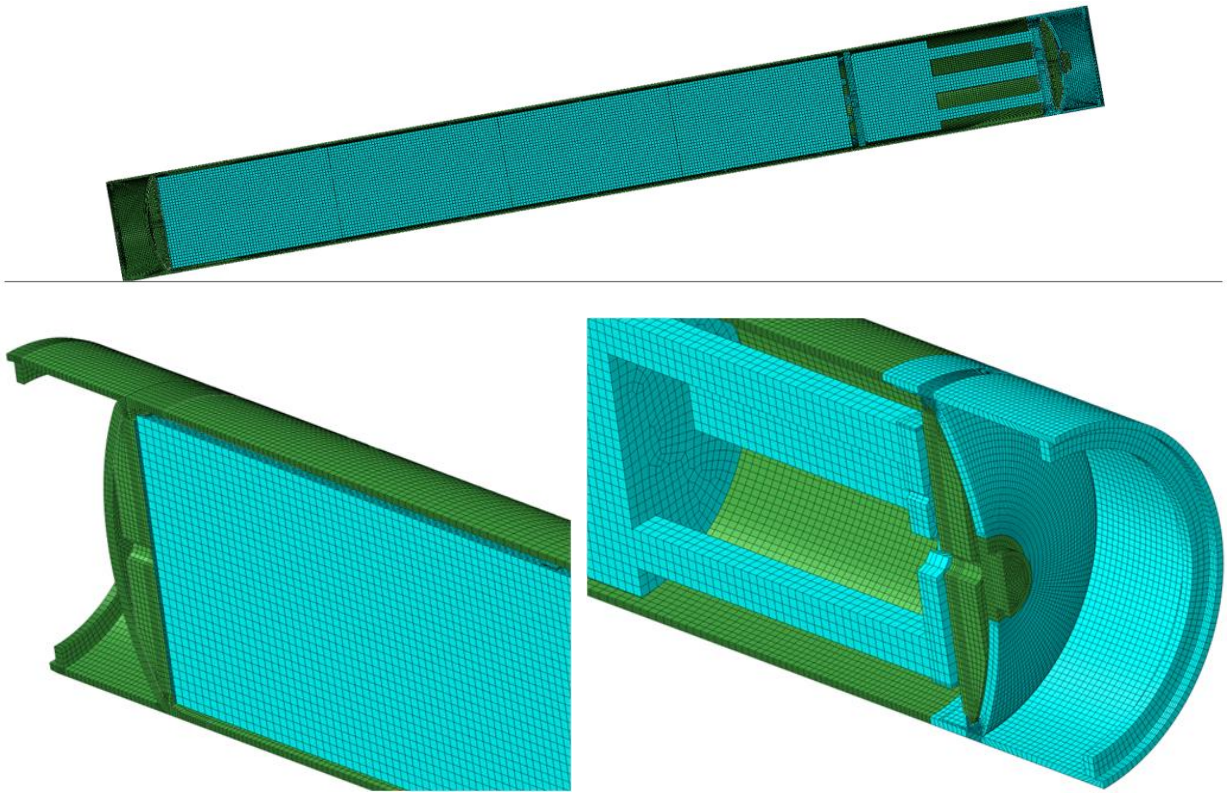

Figure 5: DOESC FEM.

Loads

The DOESC FEM assumed an internal pressure of 50 psia during the drop event, which is the DOESC's maximum allowable working pressure [6]. Based on the kinematic relationship between gravity and the 9 m drop height, an initial velocity of 13.4 m/s was assigned to the DOESC immediately prior to initial impact.

Outputs and Acceptance Criteria

Hypothetical accident conditions defined in 10 CFR 71.73 include accidental drops of SNF transportation packages. During these drop events, a large portion of kinetic energy is transformed into non-linear plastic work. These packages are required to maintain containment following the drop and severe plastic deformation. Recently, the ASME Code has defined strain-based acceptance criteria for energy-limited impact events experienced by transportation packages [26]. These acceptance criteria differ from the conventional ASME Code approach for *stress*-based acceptance criteria under worst case service conditions, which typically involves establishing limits for elastic deformation defined by the maximum shear stress theory [27].

The FEA outputs of interest in this analysis include equivalent plastic strain (output variable PEEQ in Abaqus/Explicit) and the principal stresses (σ_1, σ_2, σ_3). PEEQ is a cumulative (i.e., non-decreasing) strain measure that considers the entire deformation history, and is defined as [12, 26]:

$$\varepsilon^{pl} = \int_0^t \sqrt{\frac{2}{3}\dot{\varepsilon_{pl}} \cdot \dot{\varepsilon_{pl}}} \quad \text{(Eq. 1)}$$

However, the ASME Code's strain-based acceptance criteria do not solely consider equivalent plastic deformation. To account for triaxial loading and its effect on fracture strain for ductile materials, a stress triaxiality factor (TF) is multiplied with the equivalent plastic strain at the location under consideration. TF is defined as the ratio of hydrostatic stress to the effective (von Mises) stress:

$$TF = \frac{\sigma_1+\sigma_2+\sigma_3}{\sqrt{\frac{1}{2}[(\sigma_1-\sigma_2)^2+(\sigma_2-\sigma_3)^2+(\sigma_3-\sigma_1)^2]}} \quad \text{(Eq. 2)}$$

Per ASME Code, a minimum TF of 1 is used, which conservatively neglects potential strain hardening that occurs under compressive stress (i.e., when TF<1). The Abaqus-generated principal stresses (σ_1, σ_2, σ_3) were used to directly calculate TF. At each evaluation location, the product of equivalent plastic strain and TF (hereafter referred to as 'plastic strain product') is calculated at each time interval. There are different allowable values for the plastic strain product: averaged through the containment thickness and maximum (peak) values. These also differ depending on proximity to structural discontinuities (discussed in paragraphs FF-1141 and FF-1142 of the ASME Code's Section III Appendices). The average allowable plastic strain product is defined as:

$$\left(\varepsilon^{pl} \cdot TF\right)_{avg} \leq \begin{Bmatrix} \text{away from discontinuity (FF-1141)}, 0.67 \cdot \varepsilon_{uniform} \\ \text{near discontinuity (FF-1142)}, 0.85 \cdot \varepsilon_{uniform} \end{Bmatrix} \quad \text{(Eq. 3)}$$

The peak allowable plastic strain product for both away and near a discontinuity is:

$$\left(\varepsilon^{pl} \cdot TF\right)_{max} \leq \left\{\varepsilon_{uniform} + 0.25(\varepsilon_{fracture} - \varepsilon_{uniform})\right\} \quad \text{(Eq. 4)}$$

Where $\varepsilon_{fracture}$ is the true strain at fracture in a uniaxial tensile test and $\varepsilon_{uniform}$ is the true strain just prior to the onset of necking in a quasi-static uniaxial tensile test (Table 2). These values were obtained from previous 316L testing [13, 20]. The PEEQ and principal stress outputs were evaluated at the element's centroid. Based on 316L stainless steel data from room temperature [21], the associated allowable strain are shown in Table 2.

Table 2: ASME Code Strain Limits.

Description (Applicable ASME Code Paragraph)	**Strain Limit (mm/mm or in./in.)**
Average strain limit near discontinuity [FF-1141(a)]	0.39
Average strain limit away from discontinuity [FF-1142(a)]	0.31
Peak strain limit [FF-1421(b) and FF-142(b)]	0.83

Per ASME Code guidance, only the TF at time steps where plastic strain was occurring were used in

Equations 3 and 4. Plastic strain was defined to be occurring while the integrand of Equation 1 was increasing significantly between time steps. The accumulated plastic strain at each time step was compared to the previous time step's accumulated plastic strain. If the accumulated plastic strain was very small (< 0.0001 mm/mm or in./in.), then the TF at that time step was neglected (i.e., plastic strain product set to 0). This approach meets the intent of the ASME Code's strain-based acceptance criteria, which only considers TF during plastic deformation.

FINITE ELEMENT ANALYSIS RESULTS

FEA results from the most recently performed analysis [16] (hereafter referred to as the "original analysis") will be compared with the updated analysis and associated strain-based acceptance criteria.

Plastic Strain

Following the drop simulation, the largest plastic strain occurred in the DOESC's top head. The original analysis had the largest strains in the head, while the updated analysis showed the largest strains in the retaining ring. While these locations are in roughly the same location, the magnitude of the equivalent plastic strain is up to 160% greater in the updated analysis (Figure 6). This difference is primarily due to finer meshing of the retaining ring, slightly different dimensions of the retaining ring, and different contents in the updated analysis. When the plastic strains associated with the retaining ring are removed from the updated analysis, the equivalent plastic strain in the top head containment boundary agrees with the original analysis to within 1%. However, this only considers equivalent plastic strain, which is only one portion of the ASME Code's strain-based acceptance criteria.

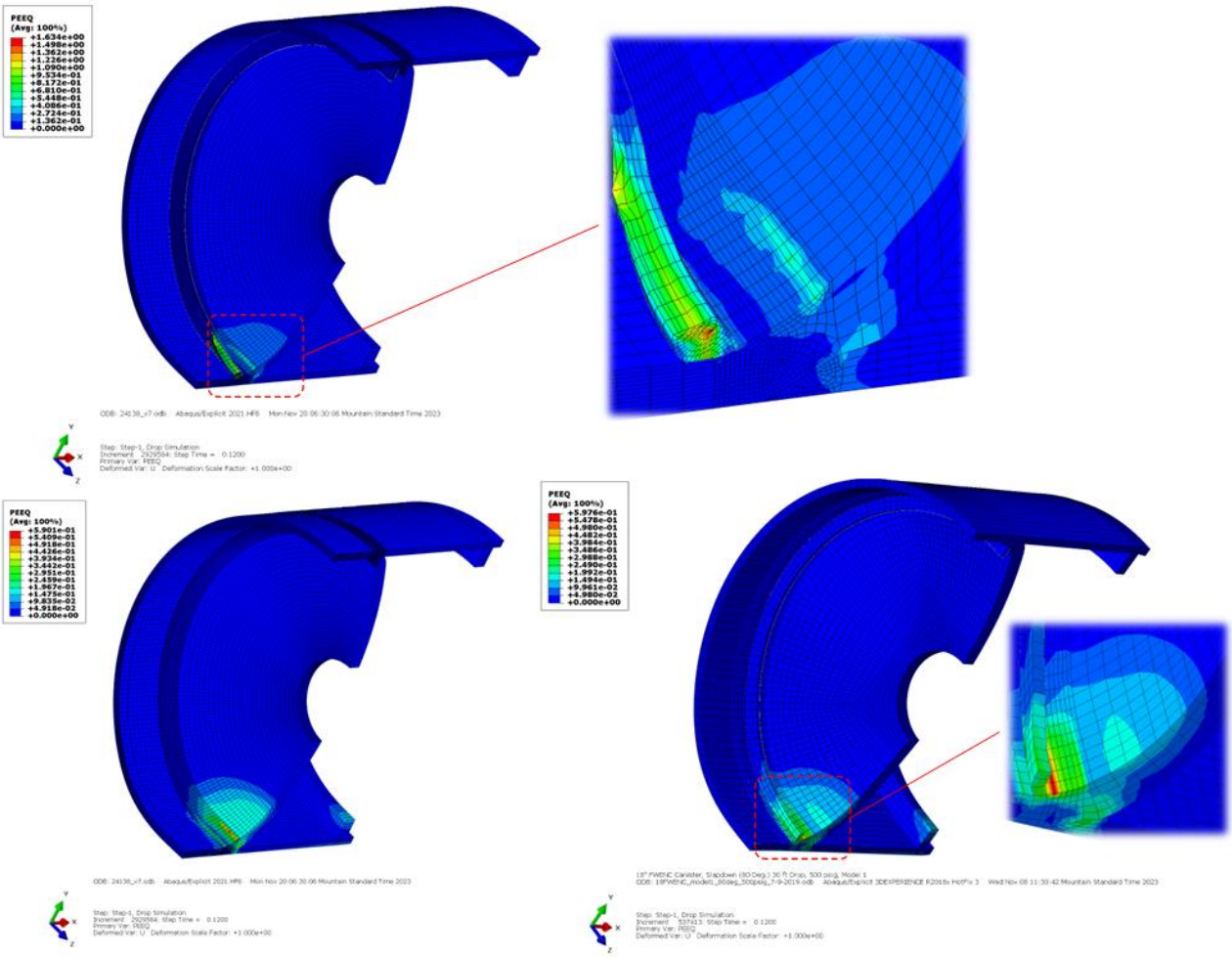

Figure 6: Plastic Deformation of Top Head With and Without Retaining Ring. Other Components Omitted for Clarity. Updated Analysis (Left) and Original Analysis (Bottom-Right).

Application of the ASME Code's Strain-Based Acceptance Criteria

As previously mentioned, no analysis of the DOESC has been performed with the ASME Code's strain-based acceptance criteria. To apply this approach, the product of the equivalent plastic strain and TF (hereafter referred to as "plastic strain product") at each element across the simulation was calculated. This value was first compared to the peak allowable strain (Equation 4). It was necessary to consider all elements across the entire simulation and not just at the end because the largest product (i.e., largest plastic deformation and stress state) is not necessarily at the end. A minimum plastic strain threshold was defined to condense the elements of interest to accelerate post-processing. This threshold was defined based on the strain limits and predicted TF across all elements during the simulation.

After the peak strains were found, these were compared to the limit in Table 2 (above). These specific elements were then queried and the thickness in their local regions were averaged, then compared to the applicable limit defined in Table 2.

Containment Evaluation

The original analysis and updated analysis showed that certain regions of the containment's Plastic strain product did exceed the peak strain limits shown above in Table 2. The original analysis showed that eight elements across the top head, main shell and bottom head exceeded the peak strain limit by up to 100%. The updated analysis showed that only elements within the top head's retaining ring exceeded the peak strain limit. Due to the refined mesh in the retaining ring, 261 elements exceeded the allowable strain. But these were limited to the retaining ring, and not the containment boundary itself.

With the original analysis, the plastic strain product in the top head averaged through the containment boundary (i.e., excluding the retaining ring) was approximately 0.26 with a peak of 1.65. For the updated analysis, the average Plastic strain product in the top head through the containment boundary was approximately 0.09 with a peak of 0.35. If the retaining ring is included, the average Plastic strain product through the thickness is 0.50 with a peak of 1.64. The locations in both the original and updated analyses of top head plastic strains were near structural discontinuities.

For the original analysis, the plastic strain product in the main shell average through the shell boundary was approximately 0.38 with a peak of 1.05. For the updated analysis, the Plastic strain product in the main shell averaged through the main shell was approximately 0.26 with a peak of 0.36. The locations in both the original and updated analyses were away from structural discontinuities.

In the original analysis, the plastic strain product in the bottom head was approximately 0.35 averaged through the thickness with a peak of 1.10. With the updated analysis, the Plastic strain product in the bottom head was approximately 0.06 average through the thickness with a peak of 0.64. The locations in both the original and updated analyses of bottom head plastic strains were near structural discontinuities.

A results comparison is presented in Table 3.

Table 3: Original and Updated FEA Results Comparison. Bolded Values Exceed ASME Code Limits from Table 2.

FEA	Component	Average (mm/mm)	Peak (mm/mm)
Original [16]	Top Head	0.26	**1.65**
	Main Shell	**0.38**	**1.05**
	Bottom Head	0.35	**1.10**
Updated	Top Head (with retaining ring)	**0.50**	**1.64**
	Top Head (without retaining ring)	0.09	0.35
	Main Shell	0.26	0.36
	Bottom Head	0.06	0.64

DISCUSSION

Results show that both the original and updated analyses contain some plastic deformation that exceed the allowable plastic strain product values. However, the updated analysis only exceeds the limits in the retaining ring, which holds the impact plate against the underside of the DOESC top head. It is considered

an attachment – not containment like the shell or heads. The strain-based acceptance criteria is not applicable to attachments, making it possibly exempt from limits of Table 2. This simply means that an alternative approach (e.g., stress-based acceptance criteria) would have to be applied to the retaining ring if strain-based acceptance criteria are not used. As Figure 6 shows, the retaining ring is deformed significantly by the impact plate during slapdown. But the strains and TF in the DOESC head are within the ASME Code's limits.

Even if the retaining ring is subject to the ASME Code's limits, additional model improvements will be made to simulate the actual material properties of the FSV fuel. Currently, the FSV fuel is modeled with a stiffness equivalent to stainless steel. This means no credit is given to the energy absorption of the graphite fuel during impact.

Although these results show some ASME Code limits are exceeded, this does not invalidate the robust design of the DOESC or imply that the DOESC containment will fail during an accidental drop. The drop-testing still demonstrates the DOESC is capable of maintaining a leaktight boundary following dropping, including with a retaining ring [12].

CONCLUSIONS

Preliminary results of the update FEA show the DOESC exceeds the average and peak strain limits set by the ASME Code. However, this is limited to the retaining ring, which is not containment material. This plastic strain is from the collision of the top impact plate with the head above the retaining ring during the slapdown drop event. Neglecting the plastic deformations of the retaining ring, the updated analysis passes ASME Code requirements throughout the entire containment. When compared to the original analysis [16], the updated analysis shows more margin above ASME Code criteria in the containment boundary.

Model refinements will be performed, including adding actual material properties for the FSV elements and modeling weld material separately. Further analysis using the conventional stress-based criteria of the Code will be pursued for components where strain-based criteria is not applicable (e.g., retaining rings). The FEA results discussed herein are preliminary. The final analysis, which will accompany the required certification for the RRDS system, will need to adhere to the guidance of the ASME Code's upcoming ASME Computational Modeling Guidance Document for Explicit Dynamics Software [25], along with any applicable regulatory requirements defined by DOE and the NRC.

Given the intent of the DOESCs to be used within a commercial transport and storage system, the 9 m free fall drop is a conservative operating load for the DOESC. The DOESC will likely experience lower decelerations and lower overall plastic work from the surrounding hardware of the transportation package. The DOESC may be relied upon for moderator exclusion, and pursuing this conservative 10 CFR 71.73 and ASME Code-based approach has its merits for RRDS.

REFERENCES

[1] U.S. Department of Energy, "Strategic Framework for DOE-Managed Spent Nuclear Fuel," Washington, D.C.,, 2021.

[2] D. A. Thomas, "DOE SNF Packaging Demonstration Overview and 2022 Activities – 23162," *WM2023 Conference Proceedings,*, 2023.

[3] D. A. Thomas, "DOE SNF Packaging Demonstration Project Overview and 2021 Activities –

22083," *WM2022 Conference Proceedings,*, 2022.
[4] L. L. Taylor, "Fort Saint Vrain HTGR (Th/U carbide) Fuel Characteristics for Disposal Criticality Analysis," Idaho National Engineering and Environmental Laboratory, Idaho Falls, ID, 2001.
[5] U.S. Nuclear Regulatory Commission, "Standard Review Plan for Transportation Packages for Spent Fuel and Radioactive Material (NUREG-2216)," Washington, D.C., 2020.
[6] U.S. Department of Energy, "Preliminary Design Specification for Department of Energy Standardized Spent Nuclear Fuel Canisters, Volume I - Design Specification," in "Volume I - Design Specification," Idaho National Engineering and Environmental Laboratory,, 1999, vol. Rev. 3, .
[7] U.S. Department of Energy, "Preliminary Design Specification for Department of Energy Standardized Spent Nuclear Fuel Canisters, Volume II - Rationale Document," in "Volume II - Rationale Document," Idaho National Engineering and Environmental Laboratory,, 1999, vol. Rev. 3, .
[8] U.S. Department of Energy, "Yucca Mountain Repository License Application," Office of Civilian Radioactive Waste Management,, 2008.
[9] (2004). *71081, Notice of Issuance of Materials License SNM–2512 for the Idaho Spent Fuel Facility*.
[10] Elmar Eidelpes, Gordon Petersen, and E. Kitcher, "Structural, Criticality, and Radiation Dose Calculations to Support SNF Loading into a DOE Standard Canister – 21113," *WM2021 Conference Proceedings,* 2021.
[11] Gordon Petersen and K. Bulmahn, "Preliminary Evaluation of the Pressure, Temperature, Flammability, and Reactivity of Peach Bottom Unit 1 and Fort Saint Vrain Spent Nuclear Fuel in a DOE Standard Canister–21285," *WM2021 Conference Proceedings*, 2021.
[12] Idaho National Laboratory, "Analytical Evaluation of the Idaho Spent Fuel Project Canister for Accidental Drop Events," Idaho Falls, ID, 2003, vol. Rev. 0.
[13] Idaho National Laboratory, "FY1999 Drop Testing Report for the 18-inch Standardized DOE SNF Canister," Idaho Falls, ID, 1999, vol. Rev. 2.
[14] *Packaging and Transport of Radioactive and Non-Nuclear Hazardous Materials*, American National Standards Institute, New York, NY, 2022.
[15] U.S. Department of Energy, "Yucca Mountain Repository Safety Analysis Report, Chapter 1: Repository Safety Before Permanent Closure," Las Vegas, NV, 2008, vol. Rev. 2.
[16] S. Snow, "Supplemental Evaluation of the DOE Standard SNF Canister for Accidental Drops," Idaho National Laboratory,, Idaho Falls, ID, 2019, vol. Rev. 0.
[17] Idaho National Laboratory, "Code of Record: Department of Energy Standard Canister," Idaho Falls, ID, 2022, vol. Rev. 0.
[18] P. Sakalaukus, N. Barrett, L. Mackey, and B. Koeppel, "Comparison of the ASME BPVC Strain-Based and Stress-Based Acceptance Criteria," in *20th International Symposium on the Packaging and Transportation of Radioactive Materials*, Juan-les-Pins, France, 2023: PATRAM22.
[19] S.-P. Kim, J. Kim, D. Sohn, H. Kwon, and M. Shin, "Stress-based vs. Strain-based safety evaluations of spent nuclear fuel transport casks in energy-limited events," *Nuclear Engineering and Design*, vol. 355, 2019.
[20] R. K. Blandford, Morton D.K., and S. D. Snow, "Tensile Stress-Strain Results for 304L and 316L Stainless Steel Plate at Temperature," in *2007 ASME Pressure Vessels and Piping Division Conference*, San Antonio, TX, 2007: American Society of Mechanical Engineers, in INL/CON-06-11962.
[21] Morton D.K. and R. K. Blandford, "Impact Tensile Testing of Stainless Steels at Various Temperatures," Idaho National Laboratory, Idaho Falls, ID, 2008.
[22] *Abaqus Version 2021.HF6*. (2021).
[23] S. D. Snow, "Software Validation Report for Abaqus Standard Explicit Version 2021.HF6 for Structural Analyses," Idaho National Laboratory, Idaho Falls, ID, 2021, vol. Rev. 0.

[24] Foster-Wheeler Environmental Corporation, "18" O.D. SNF Canister Fabrication (Long Canister)," 2002.
[25] Avallone and Baumeister, *Mark's Standard Handbook for Mechanical Engineers*, 9th ed. McGraw-Hill Book Company, 1987, p. 830.
[26] *Boiler and Pressure Vessel Code*, American Society of Mechanical Engineers, New York, NY, 2023.
[27] P. Sakalaukus, N. Barrett, and B. Koeppel, "Structural Analysis Approach for the Defense Programs Package 3 (DPP-3)," in *Proceesings of the ASME 2020 Pressure Vessels & Piping Conference*, Minneapolis, MN, 2023: American Society of Mechanical Engineers.

ACKNOWLEDGEMENTS

The authors would like to acknowledge the contribution of Nathan L. Hofmeister from Idaho National Laboratory for his assistance with modifying the finite element model(s) used for the analysis detailed herein. This research made use of Idaho National Laboratory's High Performance Computing systems located at the Collaborative Computing Center and supported by the Office of Nuclear Energy of the U.S. Department of Energy and the Nuclear Science User Facilities under Contract No. DE-AC07-05ID14517. This manuscript has been authored by Battelle Energy Alliance, LLC under Contract No. DE-AC07-05ID14517 with the U.S. Department of Energy. The U.S. Government retains and the publisher, by accepting the article for publication, acknowledges that the U.S. Government retains a nonexclusive, paid-up, irrevocable, world-wide license to publish or reproduce the published form of this manuscript, or allow others to do so, for U.S. Government purposes.